Quantifying individual (anti)bonding molecular orbitals' contributions to chemical bonding

Jurgens H. de Lange, Daniël M. E. van Niekerk and Ignacy Cukrowski*

Department of Chemistry, Faculty of Natural and Agricultural Sciences, University of Pretoria, Lynnwood Road, Hatfield, Pretoria 0002, South Africa

Correspondence to: Ignacy Cukrowski (E-mail: ignacy.cukrowski@up.ac.za)

Abstract

The shapes of molecular orbitals (MOs) in polyatomic molecules are often difficult for meaningful chemical interpretations. We report protocols to quantify contributions made by individual orbitals (molecular canonical and natural) of classical bonding, non-bonding or anti-bonding nature to (i) electron density into the inter-nuclear region and (ii) diatomic electron delocalization, *DI*(A,B). In other words, these protocols universally explain orbital's inputs to two fundamental and energy-lowering mechanisms of chemical bonding (interactions) and ease the chemical interpretation of their character in polyatomic molecules. They reveal that the MO and real-space density descriptions of the interactions are equivalent and, importantly, equally apply to all atom-pairs regardless if they are involved in a highly attractive or repulsive interaction. Hence, they not only remove ambiguity in chemical bonding interpretations (based on either MO or electron density approaches) but also demonstrate complementarity between the two such seemingly different techniques. Finally, our approach challenges some classical assumptions about MOs, such as the role of core electrons, the degree of bonding in antibonding MOs and the relative importance of frontier orbitals. Just as an example, we show that orthodox antibonding orbitals can make a significant contribution of a bonding nature to a classical covalent bond or major contribution to *DI*(A,B) of an intramolecular and highly repulsive H···H interaction.

KEYWORDS: Molecular Orbitals, Chemical Bonding, Interactions, Bond path, Quantum Chemical Topology, Molecular graph,

Introduction

Molecular Orbital (MO) theory has made invaluable contributions for decades by describing and explaining electronic structure, chemical bonding and reactivity.[1–3] Due to its importance and popularity among chemists, shapes of MOs and their energies together with electron populations can be computed in all major software packages. However, particularly when large(r) molecules are considered, '*the shapes of MOs do not easily lend themselves to meaningful chemical interpretation*'.[4] As a matter of fact, even interpretation of 'simple' diatomic molecules, such as CO, has produced different descriptions of its electronic structure in the textbooks.[5–8]

Classically, MO theory describes each MO as of *bonding* (due to the constructive overlap of atomic orbitals, AO), *nonbonding* or *antibonding* nature through investigation of their symmetry and distribution relative to the nuclear positions.[2,3] This simplistic classification of MOs, however, appeared to be insufficient and weakly (*anti*)*bonding* nature of MOs was determined from experimental photoelectron spectra[9,10] but this is generally unquantifiable[3] in polyatomic molecules. Not surprisingly, then, due to the highly delocalized nature of the orbitals (including frontier orbitals[11] or a subset of π-orbitals in conjugated molecules[2]) they are prone to misinterpretations[12–14] in polyatomic molecules.

The constructive overlap of AOs leads to a concentration of electron density in the inter-nuclear region,[2,3] thereby maximizing the attractive forces acting on nuclei in line with Feynman's theorem.[15] In addition, constructive overlap also leads to orbital expansion (delocalization), a bonding mechanism that lowers the electronic energy through either potential[16] or kinetic[17] energy driving forces. Destructive overlap of AOs, on the other hand, results in a reduction of electron density in the inter-nuclear region[2,3] but, interestingly and despite general intuition, can result in electron delocalization as well.[18] It is commonly assumed in orthodox MO-based interpretations that the core electrons do not contribute to chemical bonding and this concept is propagated in academic textbooks.[19,20] Hence, the covalent bond

order (BO) in MO theory is usually defined as a difference between the number of occupied bonding and antibonding MOs in only the valence shells.

Quantum Theory of Atoms in Molecules (QTAIM)[21] has also been fruitfully used in describing chemical bonding for decades. It is based purely on real Dirac observables, such as the molecular electron density (ED) distribution, thereby circumventing the pitfalls of MO interpretation in polyatomic molecules. QTAIM, through the use of *bond paths* (BPs) with associated *bond critical points* (BCPs) uncovers and characterises all sorts of chemical bonds. While in most cases this is in accord with general chemical knowledge and intuition,[22] QTAIM also shows BPs linking atoms seen as involved in steric repulsive interaction, *e.g.* in biphenyl.[23] This lead to a long-lasting debate about the chemical significance of BPs.[23–32] Notably, MOs were also used to interpret controversial H--H interaction[24] in biphenyl. The authors concluded that hydrogen–hydrogen bonding in planar biphenyl does not exist (due to '*Pauli (or overlap) repulsion, mainly between* C^{ortho}–H^{ortho} *phenyl MOs*'[24]) which is in direct contrast to Bader's interpretation of a bond path as '*the necessary and sufficient condition for the definition of bonding between atoms*'.[28]

The aim of this work is to reinvestigate the chemical interpretation of either canonical MOs or all natural orbitals (NOs, from post-SCF methods) through insights that can be gained from the topology of the electron density (ED) and electron delocalization patterns in real-space. From that we want to establish if it is possible to bridge the two approaches by arriving at scientifically sound and complementary orbital- and ED-based descriptions of any kind of chemical bonding. To achieve that, we developed general protocols to quantitatively interpret MO's distributions with respect to individual interatomic interactions in a molecule, thereby localizing MO interpretations to within an inter-nuclear region without the requirement of any prior mathematical localization or transformation. In order to uncover the link between the two approaches, our focus is on quantifying individual orbital contributions made to (i) the total

electron density at and in the vicinity of a *bond critical point* (BCP) on a BP (or as we prefer, a *density bridge*, DB) using our MO-ED approach and (ii) delocalisation of ED, as a number of electron-pairs for an interatomic interaction, that leads to the QTAIM-defined delocalisation index, *DI*(A,B), from which a bond order can be determined, by use of our MO-DI method. We also aim to establish whether our approach to orbital-based interpretation can be applied equally well to any kind of chemical interaction – whether attractive or repulsive (often synonymous with steric hindrance) – in any molecular structure.

Theoretical development

Full description of theoretical details relevant to the two reported MO-ED and MO-DI methods is given in Part 1 of the ESI; we provide here a brief overview of the methods.

The MO-ED method quantifies the contribution of each MO/NO to the ED along a specific vector, as well as classifies each MO/NO as concentrating, depleting or non-contributing. The total ED at any given coordinate **r** can be decomposed into orbital contributions by summing occupation-weighted orbital densities:

$$\rho(\mathbf{r}) = \sum_{i}^{N_{MO}} \nu_i |\chi_i(\mathbf{r})|^2 \qquad (1)$$

where χ_i is an MO/NO with occupation number ν_i (*e.g.* ν = 2.0 for restricted Hartree-Fock and DFT MOs). We are interested in the ED and orbital contributions related to a specific inter-nuclear region, and in particular, whether each orbital *concentrates* or *depletes* ED to this region. The second derivative of the ED is associated with electron concentration or depletion,[21] and we can therefore measure an orbital's concentration/depletion by re-expressing the Laplacian (the trace of the Hessian matrix at a given coordinate) in terms of MOs/NOs:

$$\nabla^2\rho(\mathbf{r}) = \sum_{i}^{N_{MO}} \nabla^2[\nu_i|\chi_i(\mathbf{r})|^2] \quad (2)$$

$$= \sum_{i}^{N_{MO}} \left[\frac{\partial^2\nu_i|\chi_i(\mathbf{r})|^2}{\partial x'^2} + \frac{\partial^2\nu_i|\chi_i(\mathbf{r})|^2}{\partial y'^2} + \frac{\partial^2\nu_i|\chi_i(\mathbf{r})|^2}{\partial z'^2}\right] \quad (3)$$

where x', y' and z' correspond to the eigenvectors of the Hessian matrix, and each term in Eq. 3 corresponds to the *i*th orbital's contribution to the Hessian matrix's three eigenvalues, λ_1, λ_2 and λ_3. Eq. 2 provides the net concentration/depletion of each orbital's ED contribution with $\nabla^2[\nu_i|\chi_i(\mathbf{r})|^2] \leq 0$ or ≥ 0 applying concentrating or depleting ED, respectively, and has been the subject of a previous study.[33] While informative, the individual terms in Eq. 3 can provide a more detailed description, especially with regards to individual interactions in a congested region of a molecular system. Particular importance is placed here on the MO/NO contributions to λ_2 (second term in Eq. 3) in order to link ED topology and orbital descriptions of chemical bonding: since $\lambda_1 \leq \lambda_2 \leq \lambda_3$ (by convention) and since $\lambda_1 \leq 0$ and $\lambda_3 \geq 0$ for the majority of chemical interactions (barring cage-like structures), the sign of λ_2 and associated slope are the linchpins in determining whether a DB is present or not.[29–36] The eigenvector associated with λ_2 (henceforth referred to as the λ_2–eigenvector[34,35]), and the orbital densities and partial directional second derivatives along this vector, therefore provide most information regarding the total ED's topology as well as the characters of each individual MO/NO. In conceptual terms, the λ_2–eigenvector will usually be one of the vectors perpendicular to the inter-nuclear vector, and measuring the ED or MO/NO contributions along this vector is effectively a cross-section of the inter-nuclear region. Note that while analysis along only the λ_2–eigenvector is usually sufficient, in some cases (such as in highly symmetric molecules, or when the Hessian matrix eigenvalues are degenerate) it is necessary to analyse the λ_1– or λ_3–eigenvectors as well in order to produce insights relevant to the interaction of interest.

In order to quantify orbital contributions in a consistent manner, we then measure the orbital contributions as well as partial directional second derivatives at the (3,–1) CP of an interaction, or in the absence of a DB/CP, the coordinate on an inter-nuclear vector where the ED is minimized (henceforth referred to as the minimum density point, MDP). Finally, each orbital is classified relative to its directional second derivative: orbitals with $\frac{\partial^2 v_i|\chi_i(\mathbf{r})|^2}{\partial y'^2} \leq 0$ or ≥ 0 *concentrate* or *deplete* ED, respectively, while orbitals with $v_i|\chi_i(\mathbf{r})|^2 \cong 0$ will be generally referred to as *non-contributing*.

The MO-DI method investigates the contribution of each MO/NO to the QTAIM-defined delocalization index, *DI*(A,B). *DI*s between two QTAIM-defined atomic basins are usually calculated through integration of the electron-pair density over both basins,[21]

$$\delta(\mathrm{A},\mathrm{B}) = 2\left|-\sum_{ij}\int_{\mathrm{A}} d\mathbf{r}_1 \int_{\mathrm{B}} d\mathbf{r}_2\, v_i v_j\{\chi_i^*(\mathbf{r}_1)\chi_j\ (\mathbf{r}_1)\chi_j^*(\mathbf{r}_2)\chi_i\ (\mathbf{r}_2)\}\right| \tag{4}$$

$$= 2\left|-\sum_{ij} S_{ij}^{\mathrm{A}} S_{ji}^{\mathrm{B}}\right| \tag{5}$$

for the number of electron-pairs shared by atomic basins Ω_A and Ω_B. This approach can be simplified for most wavefunctions by integrating each MO/NO pair over each atomic basin (Eq. 5), where S_{ij}^{A} is an element of the atomic overlap matrix, $S_{ij}^{\mathrm{A}} = \sum_{ij}\int_{\mathrm{A}} \sqrt{v_i}\sqrt{v_j}\chi_i^*(\mathbf{r})\chi_j(\mathbf{r})d\mathbf{r}$. We can then recover the contribution of each MO/NO to a specific *DI*(A,B) value. An approach that offers an intuitive understanding of the orbital-pair overlap in Eqs. 4 and 5 is to rewrite Eq. 5 as a delocalized density matrix,

$$D_{ij}^{(\mathrm{A},\mathrm{B})} = 2\left|-S_{ij}^{\mathrm{A}} S_{ji}^{\mathrm{B}}\right| \tag{6}$$

where the sum of all elements provides δ(A,B). The diagonal elements of this matrix, $D_{ii}^{(\mathrm{A},\mathrm{B})}$, provide each orbital's contribution to the total number of electron pairs shared between A and B.

However, the off-diagonal elements, $D_{i\neq j}^{(\mathrm{A,B})}$, provide the extent to which an orbital-pair increases delocalized electron pairs (through constructive interference) or decreases delocalized electron pairs (through deconstructive interference). Therefore, the sum of any row or column of $\mathbf{D}^{(\mathrm{A,B})}$ gives the net contribution of an orbital to the number of electron pairs shared between atoms A and B, after any orbital-pair interference effects have been taken into account. If the net contribution of an orbital is positive or negative it is therefore a result of net *constructive* or *destructive* interference with all other orbitals, and we label each orbital as such.

Computational details

All molecular systems, except Cr_2, were optimized at RHF and all-electron RCCSD levels of theory using 6-311++G(2df,2pd) as a basis set; Cr_2 was optimized at the RB3LYP/6-311++G(2df,2pd) level. All optimizations, as well as MO/NO visualizations, were performed using Gaussian 09 in conjunction with GaussView 5.[37] QTAIM and delocalization index calculations were performed using AIMAll version 19.02.13[38] together with the Müller approximation,[39] whereas IQA[40] calculations were performed using the Polestshuk's TWOe program[41] using the BBC1 approximation.[42] The CCSD/BBC1 combination has been employed because it generates IQA-defined interaction energy terms that are (i) perfectly suited for describing the nature of interactions (qualitative approach) as well as (ii) highly reliable in quantifying these interactions' strength.[43] As a matter of fact, the CCSD/BBC1 combination was used as a suitable reference to evaluate a number of (level of theory)/approximation combinations because the departure of E(IQA) from E (electronic energy of a molecule) was small (in the case of LiH dimer E has been overestimated by –3.7 kcal mol^{-1}) and it is always nearly entirely due to errors in IQA-defined self-atomic energies. Cross-sections along the λ_2–eigenvector of the ED, as well as the MO-ED and MO-DI methods, were performed using in-house codes. The XYZ coordinates of optimized molecules are given in Part 2 of the ESI.

Results and discussion

Diatomic molecules: CO, N_2, Cr_2 and H_2

A full set of data pertaining to MO-based analysis of bonding in the CO, N_2, H_2 and Cr_2 molecules at two levels of theory, all-electron CCSD and HF, is included in Parts 3, 4, 5 and 6, respectively, of the ESI. Data obtained at the CCSD level will be discussed throughout unless stated otherwise.

The highest-occupied NOs, with electron occupancy as well as their orthodox (anti)bonding labels, are shown in Fig. 1a; these NOs, each with electron occupancy close to 2*e*, correspond qualitatively to the doubly-occupied canonical MOs (CMOs) at the HF level.

The topology of the total ED along the vector perpendicular to the inter-nuclear vector (henceforth λ_2–eigenvector, Fig 1a) shows a typical feature of bonding nature, *i.e.*, a local maximum at the CP(C,O) when a DB is present (Fig. 1b), representing in this case a classical covalent bond. Concentrating ED at this CP is evidenced by the negative sign of the directional second partial derivative computed along the same eigenvector (Fig. 1c). Importantly, we note with interest that there are four out of the seven highest-occupied NOs that concentrate their individual inputs to the total ED at the CP(C,O) in the same fashion, *i.e.*, individual density contributions show local maxima and a corresponding second derivative < 0 along the λ_2–eigenvector. Both σ-bonding NOs (χ_3 and χ_4) contribute most, 28.0 and 56.6% of the total ED at the CP(C,O), respectively (Table 1) and therefore, as one would expect, they contribute to the presence of the DB. In fact, all σ-bonding orbitals in any diatomic molecule, from the quintessential σ-bond in H_2 (where $\rho(\mathbf{r}) = |\sigma_1(\mathbf{r})|^2$) to the σ-bonds in the quintuply-bonded Cr_2, exhibit this characteristic.

Unexpectedly and contrary to generally accepted views, the remaining 15 % of ED at the CP(C,O) – see Fig. 1(d) – arises from (i) χ_2 (C_{1s}, 8 %) showing that the C-atom provides its core 1*s*

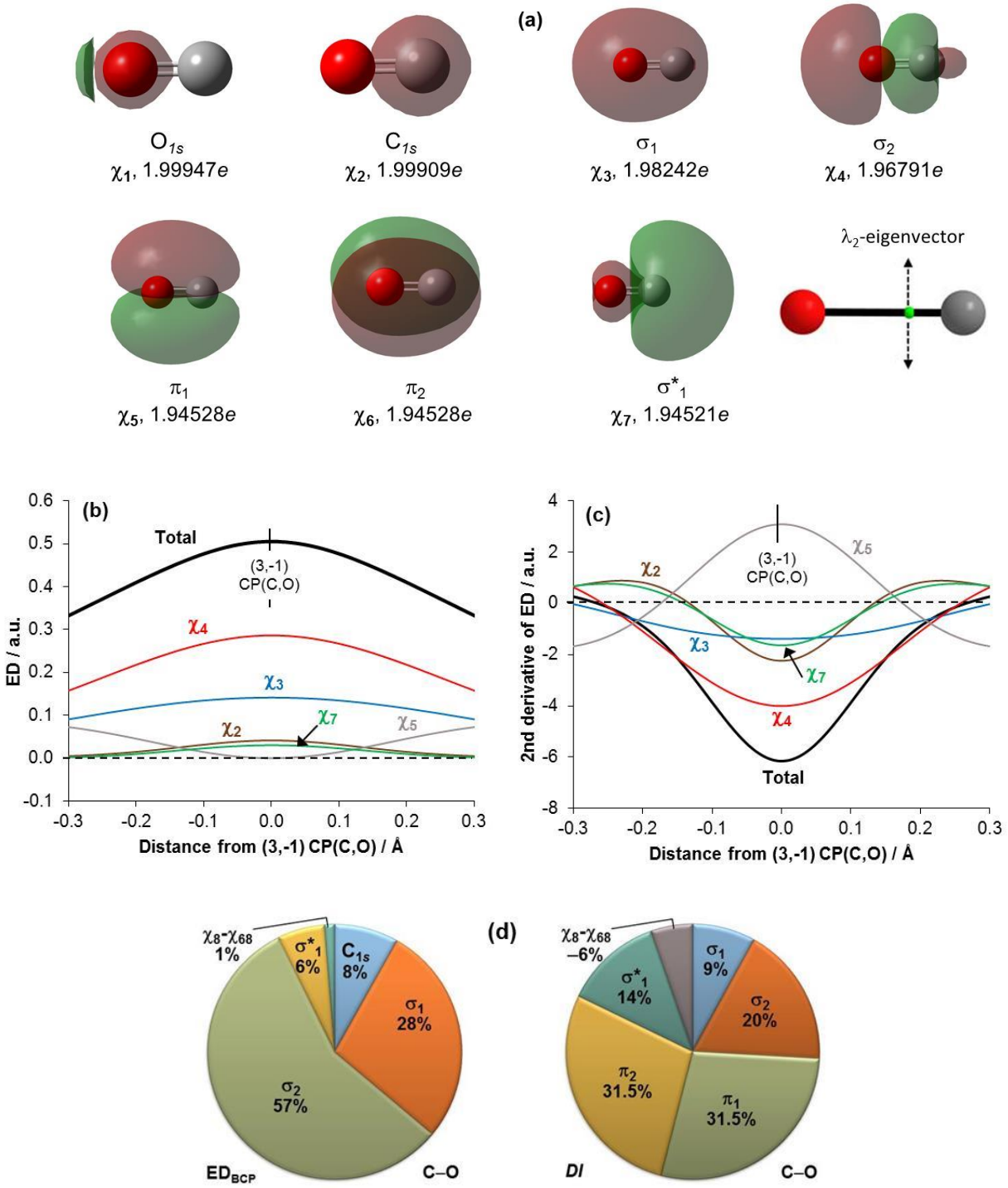

Figure 1. CCSD data obtained for the CO molecule. (a) 3D-isosurfaces (0.002 a.u. for O_{1s} and C_{1s}, 0.02 a.u. for remaining NOs) of the highest-occupied natural orbitals showing the electron occupation. A molecular graph of CO showing λ_2-eigenvector. (b) 1D cross-section along λ_2-eigenvector. (c) Directional partial second derivatives. (d) Charts showing %-contributions made to the total ED at the CP(C,O) and *DI*(C,O) by NOs.

electrons, (ii) formally classified as of antibonding nature χ_7 (σ^*_1, 7 %); this is not observed for the isoelectronic N_2 – predictably, the antibonding σ^*_1 orbital *depletes* ED, and (iii) χ_8– χ_{68} NOs that

contribute about 1%. This phenomenon in particular arises from the position of the CP, which (in the diatomic case) is determined by the relative atomic basin size difference and which, in turn, is a function of the relative polarizabilities of the atoms. It might be tempting to dismiss these observations as artefacts of the choice of measuring coordinate, but, as we shall show below, they correlate very nicely with our integrated MO-DI method. Moreover, data in Fig. 1, Table 1 and data in Part 3 of the ESI shows that CMOs computed at the HF level provide qualitatively highly comparable to that of the seven highest-occupied orbitals, all-electrons CCSD data picture. Notably, both these orbitals (χ_2 and χ_7) concentrate ED along the λ_2–eigenvector in the same fashion as χ_3 and χ_4 σ-bonding orbitals. Considering the π-bonding χ_5 and χ_6 orbitals, they play different roles along the λ_2–eigenvector. Namely, χ_5 shows a typical feature of depleting ED with local minimum in Fig. 1b at the CP(C,O) and positive sign of corresponding second derivative (Fig. 1c) whereas χ_6 makes no contribution. Exactly opposite applies to these orbitals contributions along the λ_1–eigenvector (not shown in Fig.1) and as a result they both hinder the presence of the DB as the AOs, $2p_y$ and $2p_z$ do not overlap (due to orthogonality) with $2s$.

Let us focus on QTAIM's delocalization index *DI*(A,B) that calculates the simultaneous overlap of all MOs over two atomic basins. This index has previously been suggested[44] to be a bridge between MO- and density-based approaches. For the first time (to our knowledge), we computed, using our MO-DI method, the NOs/MOs overlaps, or constructive and destructive interferences, in order to quantify their contributions to *DI*(C,O) without altering the electronic structure as others[45] have done. The delocalized density matrix (Table 2) shows the contribution of each NO and NO-pair to the total *DI*(C,O); hence, it points at the sources of the number of electron-pairs (sum of constrictive and destructive contributions) delocalised for the interatomic interaction by individual NOs. The sum of total contributions made by orbital-pairs recovers the QTAIM-defined *DI*(C,O) of 1.423 indicating that ~1.5 shared electron-pairs were contributed by

Table 1. Molecular orbital contributions and their classifications in terms of bonding in CO at the CCSD / HF (*values in italic*) levels.

		Orthodox approach		At a (3,–1) critical point CP(C,O)		Delocalisation index *DI*(C,O)	
Orbital	*N* in *e* / %-fraction *HF energy in a.u.*	Label	Classification based on AO interference	ED contribution a.u. / %-fraction	Classification based on 2nd derivative sign (λ_2)	Contribution *e*-pairs / %-fraction	Classification based on MO interference[a]
χ_1	1.9995 / 14.3 *-20.66715*	O_{1s}	nonbonding	0.00000 / 0.0 *0.00000 / 0.0*	non-contributing	0.0000 / 0.0 *0.0000 / 0.0*	non-contributing
χ_2	1.9991 / 14.3 *-11.35044*	C_{1s}	nonbonding	0.04129 / 8.2 *0.05016 / 9.3*	concentrating	0.0067 / 0.5 *0.0087 / 0.6*	constructive
χ_3	1.9824 / 14.2 *-1.54148*	σ_1	bonding	0.14132 / 28.0 *0.26415 / 48.9*	concentrating	0.1319 / 9.3 *0.2223 / 14.4*	constructive
χ_4	1.9679 / 14.1 *-0.80791*	σ_2	bonding	0.28640 / 56.6 *0.13674 / 23.3*	concentrating	0.2812 / 19.8 *0.1682 / 10.9*	constructive
χ_5	1.9453 / 13.9 *-0.65272*	π_1	bonding	0.00000 / 0.0 *0.00000 / 0.0*	depleting	0.4483 / 31.5 *0.4493 / 29.2*	constructive
χ_6	1.9453 / 13.9 *-0.65272*	π_2	bonding	0.00000 / 0.0 *0.00000 / 0.0*	depleting[b]	0.4483 / 31.5 *0.4493 / 29.2*	constructive
χ_7	1.9452 / 13.9 *-0.55263*	σ^*_1	antibonding	0.03021 / 6.0 *0.08860 / 16.4*	concentrating	0.1937 / 13.6 0.2431 / 15.8	constructive
χ_8–χ_{68}	0.2153 / 1.5	–	–	0.00641 / 1.3	–	–0.0868 / -6.1	destructive
Total	14.000 / 100.0	–	bond order = 3	0.50562 / 100.0 *0.53965 / 100.0*	DB(C,O) present	1.4234 / 100.0 1.5410 / 100.0	–

[a] positive value = constructive interference, negative value = destructive interference

[b] non-contributing orbital χ_6 is degenerate with orbital χ_5, depleting along λ_1

Table 2. Delocalized density matrix (obtained from the MO-DI approach) showing the contribution of each NO and NO-pair to the total *DI*(C,O).

NO No.	**1**	**2**	**3**	**4**	**5**	**6**	**7**	**8–68**
1	**0.00**	0.00	0.00	0.00	0.00	0.00	0.00	0.00
2	0.00	**0.01**	0.00	0.00	0.00	0.00	0.00	0.00
3	0.00	0.00	**0.24**	–0.02	0.00	0.00	–0.08	0.00
4	0.00	0.00	–0.02	**0.31**	0.00	0.00	0.00	–0.01
5	0.00	0.00	0.00	0.00	**0.50**	0.00	0.00	–0.06
6	0.00	0.00	0.00	0.00	0.00	**0.50**	0.00	–0.06
7	0.00	0.00	–0.08	0.00	0.00	0.00	**0.29**	–0.01
8–68	0.00	0.00	0.00	–0.01	–0.06	–0.06	–0.01	**0.05**
Total:	0.00	0.01	0.13	0.28	0.45	0.45	0.19	–0.09
%-fraction:	0	0	9	20	31	31	14	–6

(or can be found in) NOs that overlap constructively across C and O atomic basins. Note that the *DI*(C,O) is less than the classically expected ~3.0 shared electron-pairs, a common observation for heteropolar interactions with asymmetric orbital distributions.[18]

Data in Tables 1 and 2 leads to quite surprising observations:

(1) The σ-bonding NOs, χ_3 and χ_4, in contrast to their largest ED contributions at the CP(C,O), do not provide the majority of shared electrons as we obtained 0.132 (9%) and 0.281 (20%) electron-pairs, respectively. Notably, similar %-ratio, *i.e.*, $(\chi_4/\chi_3)_{\%\text{-contribution}}$ of about 2, is observed for both contributions, ED at the CP(C,O) and electron-pairs shared in the inter-nuclear C···O region.

(2) The π-bonding NOs χ_5 and χ_6 (they deplete ED at the CP(C,O)) provide the largest contributions to the *DI*(C,O) as they share 0.448 (31.5%) electron-pairs each.

(3) The σ-antibonding χ_7 shares more electrons than the highest-occupied σ-bonding NO (χ_3), namely 0.194 (14 %) electron-pairs. In stark contrast, the equivalent antibonding σ^*_1 orbital of N_2 contributes just 0.019 of a total 2.32 electron-pairs (*i.e.* 1%).

Table 1 compares the CCSD and HF data as well as contrasts the orthodox classification against our approaches in interpreting NOs/MOs roles played in terms of their contribution toward the C–O covalent bond. Notably, the overall qualitative, either CCSD- or HF-based,

picture is the same. It shows that there is no obvious correlation between a classical classification of NOs/MOs (as *bonding*, *antibonding*, *nonbonding*) and their contributions to the ED at the CP(C,O) or to *DI*(C,O); many surprising discrepancies were mentioned already above. Importantly, when adhering to classical nomenclature, data in Table 1 clearly shows that the antibonding NO/MO χ_7 in CO is better described as of weak antibonding nature as it does concentrate ED in the inter-nuclear region and contribute to *DI*(C,O) due to the constructive orbital overlap over both atomic basins. This finding, obtained from the MO-ED protocol, correlates perfectly well with interpretations arrived at from experimental data[9,10] and by considering the heteropolarity of the molecule.[46] The equivalent antibonding σ^*_1 (χ_5) orbital in N_2 does not concentrate ED in the inter-nuclear region but slightly contributes (0.8% at CCSD) to *DI*(N,N) hence to the covalent bond formation. If so, can one describe this orbital as being almost of pure antibonding nature?

Academic textbooks[2,3] teach us that highest occupied bonding MOs contribute most toward chemical bonding. Through the MO-DI protocol (leading to uncover MO interference) we not only recovered this notion but also quantified MO's contributions to *DI*(A,B). At the same time, the MO-ED protocol, through quantifying individual MOs contributions to the total ED at a CP(A,B), shows that non-electron-pair sharing orbitals concentrate density most, hence constitute the ρ_{BCP} quantity that is commonly used to decide on the open or closed shell character of an interaction/bond.[47] Clearly, more systems must be studied to establish if this observation is of general nature.

To summarise, the MO-ED results for diatomic molecules revealed that all σ-bonding and σ*-antibonding orbitals with some of a σ-bonding character (*e.g.* the *weak* antibonding orbital σ^*_1 in CO), concentrate ED in the inter-nuclear region and therefore contribute to a DB's presence. π-bonding and pure nonbonding orbitals (*e.g.* O_{1s} in CO) either deplete or do not contribute ED in the inter-nuclear region; they hinder the presence of a DB. We also noted that

pure antibonding orbitals (*e.g.* σ^*_1 in N_2) do not contribute any ED and might not facilitate nor hinder the presence of a DB.

LiH dimer (Li_2H_2)

Li_2H_2 presents a very interesting, polyatomic case study for MO interpretation – full data set is included in Part 7 of the ESI. There are two bonding and antibonding CMO pairs (with 2*e* each at HF) with one pair originating from a coupling between fully-occupied Li_{1s} atomic orbitals and the other from a coupling between fully-occupied H_{1s} atomic orbitals if all atomic orbitals are allowed to mix simultaneously.

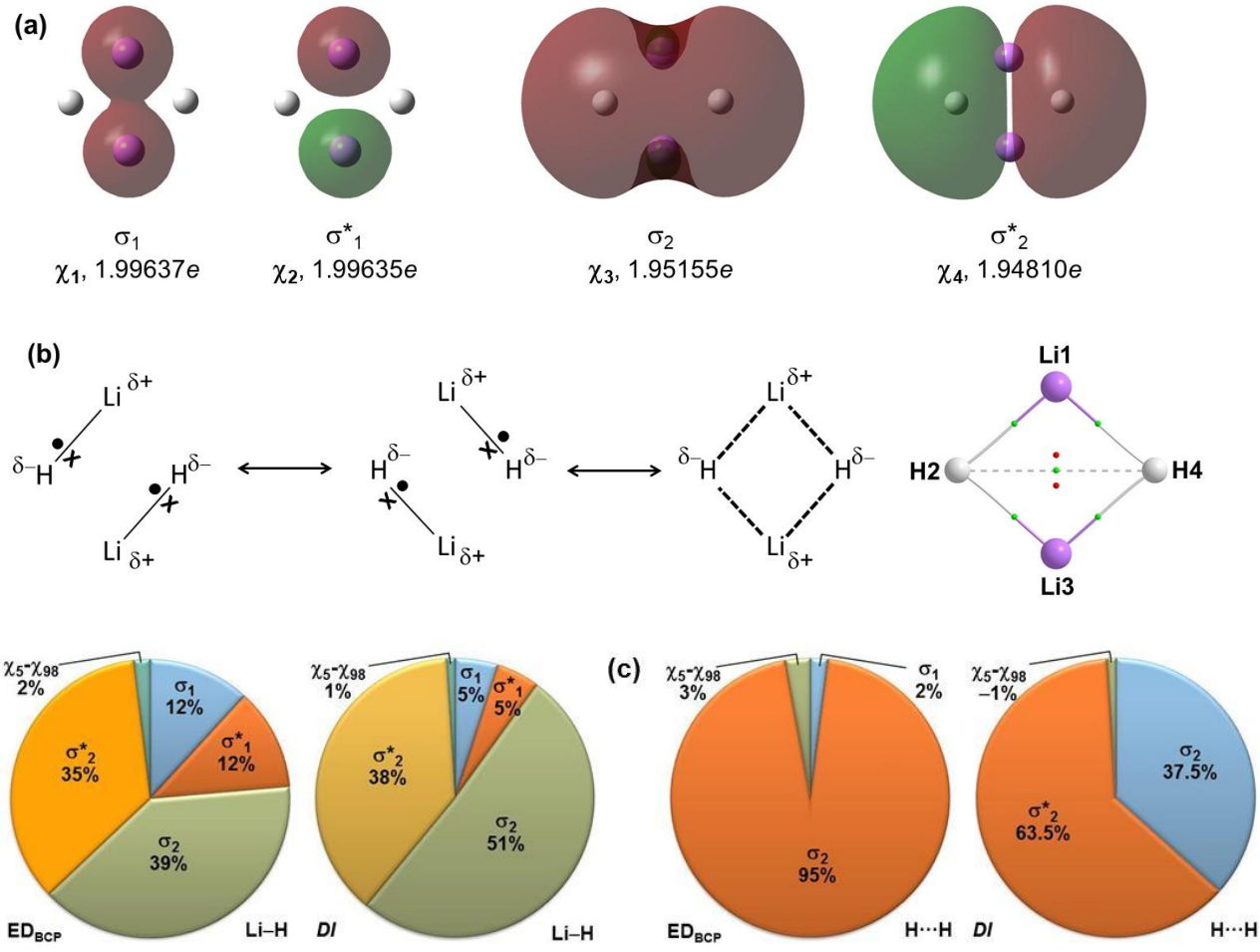

Figure 2. Part (a) – 3D-isosurfaces (0.02 a.u.) of the highest-occupied NOs also showing the electron occupations (CCSD data) obtained for LiH dimer. Pat (b) – Lewis resonance structures and a molecular graph of the dimer showing DBs; bond and ring critical points as green and red spheres, respectively. (c) Charts showing %-contributions made to the total ED at the CP(Li,H)/CP(H,H) and *DI*(Li,H)/*DI*(H,H) by NOs.

Qualitatively comparable four highest occupied NOs (Fig. 2a) were computed at CCSD (among the total number of 98) and they contain 98% of the total electron count. Hence, from a classical point of view, the resultant bond order = 0 indicates that there are no covalent bonds in the LiH dimer. This fully agrees with dominance of the interacting quantum atoms (IQA)[40] classical electrostatic Coulomb interaction terms: $V_{cl}^{Li,H}$, $V_{cl}^{H,H}$ and $V_{cl}^{Li,Li}$ of –146.0, +99.5 and +118.5 kcal mol^{-1} – Table 3.

Table 3. CCSD and HF (*in italic*) data obtained for LiH dimer. Part a: Orbitals' electron populations at CCSD (*N*) / HF energies and their orthodox classification. Part b: IQA-defined diatomic interaction energy ($E_{int}^{A,B}$) and its classical electrostatic Coulomb ($V_{cl}^{A,B}$) and exchange-correlation ($V_{XC}^{A,B}$, the interaction energy due to purely quantum effects) components. Interatomic distances, d(A,B), are also provided.

Part a		Orthodox approach	
Orbital	*N* in *e* / %-fraction *HF energy in a.u.*	Label	Classification based on AO interference
χ_1	1.9964 / 25.0 *–2.40826*	σ_1	bonding
χ_2	1.9964 / 25.0 *–2.40607*	σ^*_1	antibonding
χ_3	1.9516 / 24.4 *–0.37163*	σ_2	bonding
χ_4	1.9481 / 24.4 *–0.31887*	σ^*_2	antibonding
χ_5–χ_{98}	0.1076 / 1.3	–	–
Total	8.000*e*	–	bond order = 0

Part b			Interaction energy and its components (in kcal mol^{-1})		
Atoms		d(A,B)			
A	B	(in Å)	$E_{int}^{A,B}$	$V_{cl}^{A,B}$	$V_{XC}^{A,B}$
Li	H	1.7487	–160.6	–146.0	–14.5
H	H	2.6728	86.1	99.5	–13.4
Li	Li	2.2557	117.5	118.5	–1.0

In order to obtain quantified individual orbitals contributions at relevant CPs and uncover the orbital-based origin (if any) of the presence/absence of DBs, we applied the MO-ED method to three unique inter-nuclear regions with the appropriate λ-eigenvectors passing through the

CP(Li,H), CP(H,H) and a minimum density point MDP(Li,Li) between Li-atoms as they are not linked by a DB. Result obtained for the total ED curve, computed for the Li,H atom-pair (Fig. 3a), shows the same principle feature as observed for all investigated diatomic molecules with a classical covalent bond. It is then clear that the trend in the total ED, when a DB is present, is not related to most general classification of bonds as covalent or ionic; Li and H atoms, due to large difference in their net atomic charges of 1.80*e* are involved in highly attractive and dominating electrostatic interaction. Contrary to classical thinking, all highest occupied NOs (from χ_1 to χ_4, two bonding and two antibonding) do concentrate ED as all directional partial second derivatives, computed for individual orbital's contributions in the vicinity (±0.3 Å) of CPs(Li,H), are negative (Fig. 3b). Moreover, both the bonding (χ_3) and antibonding (χ_4) orbitals contribute to the DB(Li,H) presence nearly equally, on average ~37.2±2% (Fig. 2c). The same observation applies to 1*s* core bonding χ_1 and antibonding χ_2 orbitals centred on the Li-atoms, but their contributions are 3-times smaller, 11.8% each; notably, traces of their individual contributions resemble that of the total ED. The remaining χ_5–χ_{98} NOs made an overall constructive, or of bonding nature, contribution of 1.9% at the CPs(Li,H). Finally, in accord with classical thinking when the orthodox nature of orbitals is ignored, the higher-energy χ_3 and χ_4 CMOs (at HF) and their counterpart NOs (at CCSD) contribute most to ED at four CPs(Li,H) – Table 4.

It is gratifying to note that the overall feature of the total ED curve, Fig. 3c (obtained for the H,H atom-pair involved in highly repulsive electrostatic interaction of +86.1 kcal mol^{-1}) is as observed for the Li,H atom-pair. In the case of the H···H interaction, however, only one σ_2-bonding NO (χ_3) concentrates ED and this correlates perfectly well with the shape of this NO that is centred on the two H-atoms. Furthermore, one might have assumed that if a DB is present in this case then the main contribution should have come from the ED-rich H-atoms. Data in Fig.3d shows that χ_1 and χ_2 centred on the Li-atoms deplete ED at the CP(H,H) as the relevant

partial directional second derivatives are positive. The antibonding χ_4 does not make any input; hence, it does not deplete ED at the CP(H,H).

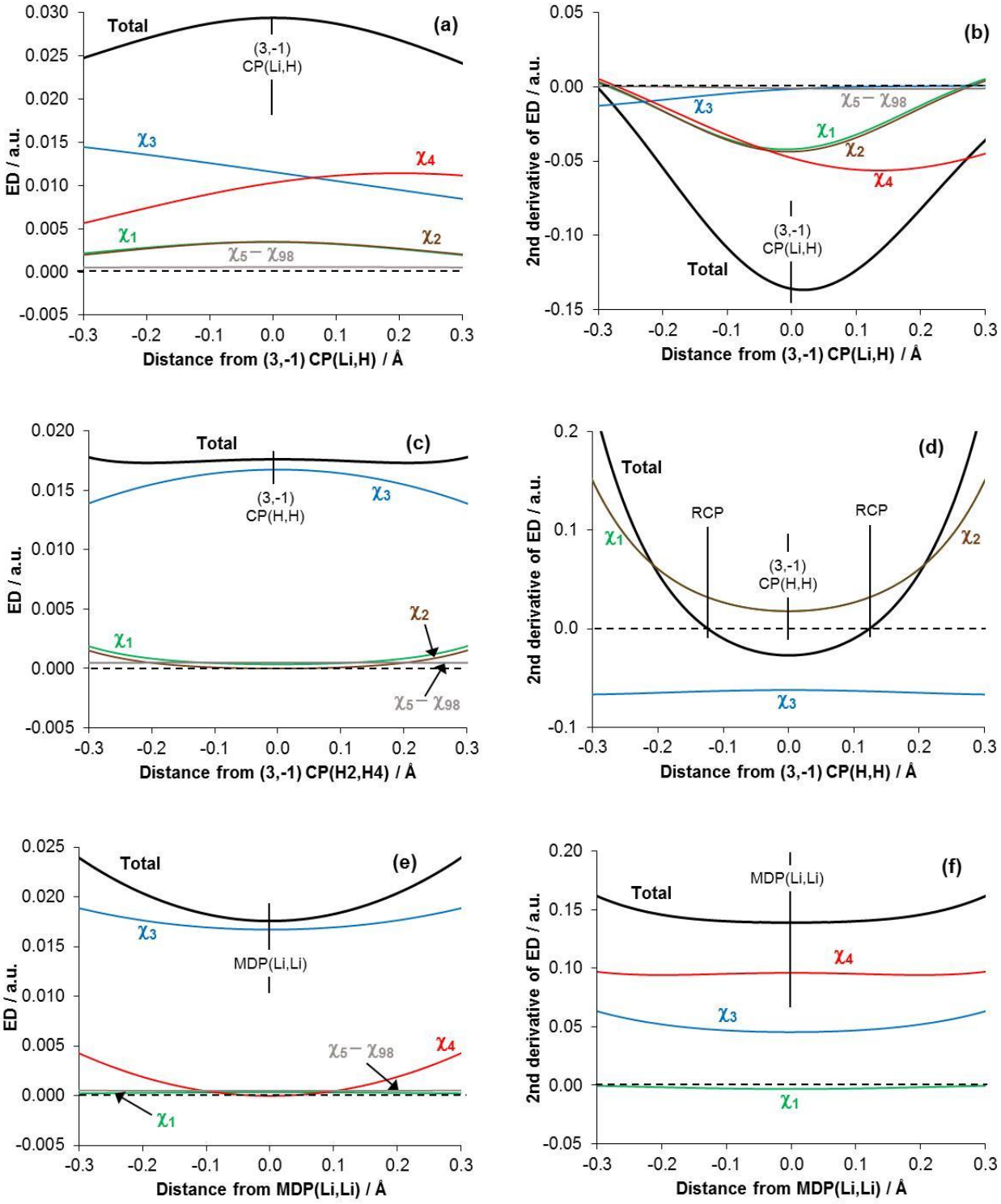

Figure 3. CCSD data obtained for Li···H, H···H and Li···Li inter-nuclear regions in the LiH dimer using the MO-ED method. Trends in the orbital-attributed ED in close proximity (±0.3 Å) to the specified points (CPs and MDP) computed from a 1D cross-section along appropriate λ-eigenvectors and directional partial second derivatives computed on these trends.

Table 4. CCSD and HF (*in italic*) data obtained for LiH dimer. NOs and MOs contributions to ED at CP(Li,H), CP(H,H) and MDP(Li,Li) and orbitals electron-pair contributions to *DI*(A,B).

	At critical / minimum density point		Delocalisation index	
Orbital	ED contribution a.u. / %-fraction	Classification based on 2nd derivative sign (λ_2)	Contribution *e*-pairs / %-fraction	Classification based on MO interference[a]
Li···H interaction				
χ_1	0.00347 / 11.8 *0.00366 / 12.5*	concentrating	0.0050 / 4.5 *0.0052 / 4.6*	constructive
χ_2	0.00347 / 11.8 *0.00345 / 11.8*	concentrating	0.0057 / 5.0 *0.0058 / 5.1*	constructive
χ_3	0.01156 / 39.4 *0.01157 / 39.5*	concentrating	0.0578 / 51.3 *0.0587 / 51.7*	constructive
χ_4	0.01032 / 35.1 *0.01060 / 36.2*	concentrating	0.0432 / 38.3 *0.0438 / 38.6*	constructive
χ_5–χ_{98}	0.00056 / 1.9	–	0.0010 / 0.9	constructive
Total	0.02938 a.u. *0.02938* a.u.	CP(Li,H) present	0.1126 *e*-pairs *0.1134 e*-pairs	–
H···H interaction				
χ_1	0.00036 / 2.0 *0.00043 / 2.5*	depleting	0.00046 / 0.5 *0.00068 / 0.7*	constructive
χ_2	0.00000 / 0.0 *0.00000 / 0.0*	depleting	0.00003 / 0.0 *0.00003 /0.0*	constructive
χ_3	0.01674 / 95.1 *0.01682 / 97.5*	concentrating	0.03658 / 37.4 *0.03658 / 33.9*	constructive
χ_4	0.00000 / 0.0 *0.00000 / 0.0*	non-contributing	0.06192 / 63.4 *0.06192 / 65.4*	constructive
χ_5–χ_{98}	0.00051 / 2.9	–	–0.00131 / –1.3	destructive
Total	0.01760 a.u. *0.01725* a.u.	CP(H,H) present	0.09768 *e*-pairs *0.09768 e*-pairs	–
Li···Li interaction				
χ_1	0.00036 / 2.0 *0.00043 / 2.5*	concentrating	0.00064 / 9.9 *0.00061 / 9.8*	constructive
χ_2	0.00000 / 0.0 *0.00000 / 0.0*	non-contributing	–0.00062 / –9.5 *–0.00066 / –10.6*	destructive
χ_3	0.01674 / 95.1 *0.01682 / 97.5*	depleting	0.00434 / 66.9 *0.00415 / 66.8*	constructive
χ_4	0.00000 / 0.0 *0.00000 / 0.0*	depleting	0.00207 / 31.8 *0.00210 / 33.9*	constructive
χ_5–χ_{98}	0.00051 / 2.9	–	0.00006 / 0.9	constructive
Total	0.01760 a.u. *0.01725* a.u.	CP(Li,Li) absent	0.00649 *e*-pairs *0.00629 e*-pairs	–

Finally, Figs. 3e and 3f illustrate the same NOs contributions to and around the MDP(Li,Li) that fully explain why a DB is not present between the Li-atoms. The trend in the total ED is (i) exactly opposite to what we found for all investigated covalent bonds and the LiH and H,H atom-pairs and (ii) typical for atoms that are not linked by a DB; a minimum in ED at the MDP(Li,Li) is seen and the second derivative computed for this trace is positive meaning that the overall effect is depleting ED in this region. Interestingly, the χ_1 bonding NO (representing core electrons of Li) slightly concentrates ED (the corresponding second derivative in Fig. 3f is negative in the vicinity of and at the MDP(Li,Li)) but this is compensated over by χ_3 NO, which is highly depleting in this inter-nuclear region (this bonding orbital concentrates ED for the H,H atom-pair).

Delocalized ED matrices (Table 5), computed using the MO-DI methodology, reveal quite unexpected trends, namely:

(1) The H-atoms centred bonding χ_3 and antibonding χ_4 NOs contribute most to *DI*(Li,H) = 0.11, 51 and 38%, respectively. The Li-centred bonding χ_1 and antibonding χ_2 NOs, containing core 1*s* electrons, also delocalise ED with ~5% contributions – Fig. 2c.

(2) The same χ_3 and χ_4 orbitals, but in the reverse order, contribute to the *DI*(H,H), 63(χ_4) and 37(χ_3)%. As we noticed for bonding-antibonding orbital-pairs in diatomic molecules, χ_3 and χ_4, due to large destructive interference between them, reduced the number of *e*-pairs shared between H-atoms by a large value of 0.82 resulting in a net *DI*(H,H) = 0.10.

(3) Destructive interference between the Li-centred bonding-antibonding pair χ_1 and χ_2 resulted in a complete cancellation of their 0.001 and –0.001 *e*-pair contributions to *DI*(Li,Li). A small *DI*(Li,Li) of 0.006 is predominantly due to H-centred χ_3 and χ_4 that delocalised 0.004 and 0.002 *e*-pairs, respectively.

Table 5. Delocalized ED matrices showing the contribution of each NO and NO-pair to the total *DI*(A,B) computed for three unique interactions in LiH dimer using the MO-DI methodology.

	Li···H interaction				
NO No.	**1**	**2**	**3**	**4**	**5–98**
1	**0.01**	0.00	0.00	0.00	0.00
2	0.00	**0.01**	0.00	0.00	0.00
3	0.00	0.00	**0.06**	0.00	0.00
4	0.00	0.00	0.00	**0.04**	0.00
5–98	0.00	0.00	0.00	0.00	**0.00**
Sum	0.01	0.01	0.06	0.04	0.00
%	4	5	51	38	1
	H···H interaction				
1	**0.00**	0.00	0.00	0.00	0.00
2	0.00	**0.00**	0.00	0.00	0.00
3	0.00	0.00	**0.85**	–0.82	0.00
4	0.00	0.00	–0.82	**0.88**	–0.01
5–98	0.00	0.00	0.00	–0.01	**0.00**
Sum	0.00	0.00	0.04	0.06	0.00
%	0	0	37	63	–1
	Li···Li interaction				
1	**0.986**	–0.986	0.001	0.000	0.000
2	–0.986	**0.987**	–0.001	0.000	0.000
3	0.001	–0.001	**0.004**	0.000	0.000
4	0.000	0.000	0.000	**0.002**	0.000
5–98	0.000	0.000	0.000	0.000	**0.000**
Sum	0.001	–0.001	0.004	0.002	0.000
%	10	–10	67	32	1

Importantly, and as one would expect,[45,48–50] the MO-DI-based results correlate perfectly well with the diatomic interaction energy due to purely quantum effects, *i.e.*, the IQA exchange-correlation $V_{XC}^{A,B}$ component of the total diatomic interaction energy $E_{int}^{A,B}$ ($V_{XC}^{A,B}$ is used to quantify a covalent component in chemical bonding) when normalised by the inter-nuclear distance d(A,B). To this effect, we obtained *DI*(A,B), using the BBC1 approximation, of 0.115, 0.174 and 0.012 *e*-pairs (after normalisation one obtains *DI*(A,B)/d(A,B) of 0.066, 0.065 and 0.005, respectively) and $V_{XC}^{A,B}$ of –14.53, –13.42 and –0.96 kcal mol^{-1} for the Li···H, H···H and Li···Li interactions, respectively. Notably, comparable *DI*(A,B)/d(A,B) and $V_{XC}^{A,B}$ values were

obtained for non-controversial (Li···H) and highly controversial (H···H) interactions, both exhibiting a DB.

What is then the relationship between orbitals and the topology of the ED from a chemistry perspective? Our interpretation is as follows.

Focusing on the MO-ED approach, it explains why each DB is present/absent in the LiH dimer used here as an example. Moreover, it provides the origin of this topological phenomenon in terms of MOs and CMOs contributions; notably, the presence or absence of these DBs, the H···H DB including, cannot be explained by recently suggested criterion.[51] In polyatomic Li_2H_2, two pairs of (anti)bonding σ-orbitals either concentrate or deplete or make no contribution to ED in three inter-nuclear regions. The degree of σ-bonding character of an orbital can be established by quantifying its ED contribution to any given interatomic interaction in a polyatomic molecule. From all the above observations it also follows that a DB presence/absence can be rigorously and quantitatively explained by accounting for concentrating (by σ-bonding and weak σ*-antibonding orbitals) and depleting (pure σ*-antibonding and π-bonding) ED contributions made by all orbitals to a specific inter-nuclear region. Notably and importantly, the presence or absence of a DB, as well as the degree of σ-bonding character, is not linked with the attractive/repulsive nature of a diatomic interaction.

The MO-DI method shows that both bonding and antibonding orbitals can contribute to the electrons shared by two atoms, *i.e.* to *DI*(A,B). However, the resultant or net *DI*(A,B) is determined by the sum of constructive and deconstructive interferences between the molecular orbitals as recovered from the MO-DI approach. In some cases, two orbitals' contributions cancel off completely (*e.g.*, considering a typical bonding-antibonding pair χ_1 and χ_2 in N_2 and for the Li,Li interaction in Li_2H_2) but correlations between *all* orbitals generally result in the net *DI*(A,B) > 0. Hence, the bonding character of any given orbital, in terms of *DI*(A,B), is therefore only revealed when considering the correlations between all other orbitals.

From *DI*(A,B) being correlated with always negative $V_{XC}^{A,B}$ it follows that a net *DI*(A,B) strengthens an interaction; the larger *DI*(A,B) the stronger bonding interaction and this correlates well with, *e.g.*, triple covalent bond being stronger than double or single bond. Moreover, we note that in all cases when the orbitals concentrated ED such that a DB was present, they also contributed to electron sharing (despite the presence of some destructive interference) and stabilization *via* $V_{XC}^{A,B}$. Going beyond molecules studied here, a C–C bonding interaction (representing a single classical covalent bond) is made of $V_{cl}^{A,B} > 0$ but $V_{XC}^{A,B} << 0$, whereas H···H in Li_2H_2 is characterized by $V_{cl}^{A,B} >> 0$ and $V_{XC}^{A,B} < 0$. However, the underlying electronic mechanisms, and the energetic consequence of the DB presence between the atoms, are the same. Clearly, the MO and real-space density descriptions of the interactions are equivalent – that of a bonding contribution to an interaction.

Conclusions

To conclude, the bonding characteristics of any given orbital can be determined in di- and poly-atomic molecular systems through investigation of two energy-lowering mechanisms: concentration of ED in an inter-nuclear A···B region (when A and B share an interatomic surface) and net contribution to electron delocalization, *DI*(A,B), for any atom-pair. Such approaches provide chemists with quantifiable, transferable and scalable knowledge of orbitals with respect to chemical bonding, as opposed to the qualitative classical methods of isosurface investigation and atomic orbital correlations. We also note that these insights are conveniently captured by the presence of a DB: while the presence of a DB does not imply that the atom-pair A,B is bonded, it does imply an interaction with some degree of bonding character. Hence, Bader's view that the presence of a BP is '*the necessary and sufficient condition for the definition of bonding between atoms*'[22] holds but only when it refers to just a covalent contribution made to the interaction and not to its overall nature: either attractive – perceived as

a manifestation of chemical bonding, or repulsive – interpreted as *e.g.* destabilising steric hindrance.

Finally, this work shows that the degree of (anti)bonding character of orbitals and their qualitative contributions depend highly on an atom-pair considered and its placement in a molecular environment. Clearly it would be highly informative and beneficial to chemists' community at large if the roles played and their contributions made (to any interatomic interaction) by individual MOs/NOs in molecules were easily available as this should assist in better understanding of chemical reactivity or catalytic properties, to mention but a few. Our methods also fully capture one of the intrinsic advantages of MO theory – its ability to describe delocalized electrons, aromaticity and multi-centre interactions – and fully cast it into a convenient diatomic view of chemistry. It is then our hope that, due to the relative simplicity and demonstrated potential, the MO-ED and MO-DI methods reported here will be incorporated in commercial software soon.

Conflict of interest

There are no conflicts to declare.

Acknowledgment

The authors gratefully acknowledge the Centre for High Performance Computing (CHPC), South Africa, for providing computational resources to this research project and National Research Foundation of South Africa, Grant Number 105855, for financial support.

References

1. F. M. Bickelhaupt and E. J. Baerends, *Reviews in Computational Chemistry*, Wiley-VCH, New York, 2000.
2. P. Atkins and R. Friedman, *Molecular Quantum Mechanics, Fourth Ed.* Oxford University Press, New York, 2005.

3. I. N. Levine, *Quantum Chemistry Seventh Ed.* Pearson Education Inc., New York, 2009.
4. R. D. Hancock and I. V. Nikolayenko, *J. Phys. Chem. A*, 2012, **116**, 8572–8583.
5. Y. Liu, B. Liu, Y. Liu and M. G. B. Drew, *J. Chem. Educ.*, 2012, **89**, 355−359.
6. J. N. Murrell, S. F. Kettle and J. M. Tedder, *The Chemical Bond, Second Ed.* Wiley-VCH, New York, 1985.
7. A. G. Whittaker, A. R. Mount and M. R. Heal, *Instant Notes Physical Chemistry,* BIOS Scientific Publishers Limited, Oxford, 2000.
8. P. A. Cox, *Instant Notes Inorganic Chemistry,* BIOS Scientific Publishers Limited, Oxford, 2000.
9. J. L. Gardner and J. A. R. Samson, *J. Chem. Phys.*, 1975, **62**, 1447−1452.
10. G. Zhou and L. Duan, *Fundamentals of Structural Chemistry (JiegouHuaxue Jichu), in Chinese, Fourth Ed.,* Peking University Press, Beijing, 2008.
11. K. Fukui, T. Yonezawa and H. Shingu, *J Chem Phys,* 1952, **20**,722–725.
12. F. Weinhold and C. R. Landis, *Chem. Educ. Res. Pract.*, 2001, **2,** 91–104.
13. R. S. Mulliken, *Science,* 1967, **157**, 13.
14. F. Weinhold and C. R. Landis, *Valency and Bonding: A Natural Bond Orbital Donor-Acceptor Perspective,* Cambridge UK Press, Cambridge, 2005.
15. R. P. Feynman, *Phys. Rev.,* 1939, **56**, 340–343.
16. J.C. Slater, *Quantum Theory of Molecules and Solids, Vol. 1,* McGraw-Hill, New York, 1963.
17. K. Ruedenberg and M. W. Schmidt, *J. Phys. Chem. A.*, 2009, **113**, 1954–1968.
18. A. M. Pendás, E. Francisco, *ChemPhysChem*, 2019, DOI:10.1002/cphc.201900641.
19. D. F. Shriver, P. W. Atkins and C. H. Langford, *Inorganic Chemistry, Second Ed.*, Oxford University Press, Oxford, 1994.
20. J. E. Huheey, E. A. Keiter and R. L. Keiter, *Inorganic Chemistry, principles of structure and reactivity, Fourth Ed*, Prentice Hall, Upper Saddle River, 1993.
21. R. F. W. Bader, *Atoms in molecules: A Quantum Theory,* Oxford University Press, Oxford, 1990.
22. R. F. W. Bader, *J. Phys. Chem. A,* 1998, **102**, 7314–7323.
23. C. F. Matta, J. Hernandez-Trujillo, T-H. Tang and R. F. W. Bader, *Chem. Eur. J.*, 2003, **9**, 1940–1951.
24. J. Poater, M. Solà and F. M. Bickelhaupt, *Chem. Eur. J.*, 2006, **12**, 2889–2895.
25. J. Poater, M. Solà and F. M. Bickelhaupt, *Chem. Eur. J.*, 2006, **12**, 2902–2905.
26. J. Poater, M. Solà and F. M. Bickelhaupt, *J. Org. Chem.*, 2007, **72**, 1134–1142.

27. R. F. W. Bader, *J. Phys. Chem. A*, 2009, **113**, 10391–10396.
28. R. F. W. Bader, *Chem. Eur. J.*, 2006, **12**, 2896–2901.
29. C. Foroutan-Nejad, S. Shahbazian and R. Marek, *Chem. Eur. J.*, 2014, **20**, 10140–10152.
30. Z. A. Keyvani, S. Shahbazian and M. Zahedi, *Chem. Eur. J.*, 2016, **22**, 5003–5009.
31. Z. A. Keyvani, S. Shahbazian and M. Zahedi, *ChemPhysChem*, 2016, **17**, 1–10.
32. S. Shahbazian, *Chem. Eur. J.*, 2018, **24**, 5401–5405.
33. J. Reinhold, O. Kluge and C. Mealli, *Inorg. Chem.*, 2007, **46**, 7142–7147.
34. I. Cukrowski, J. H. de Lange, A. S. Adeyinka and P. Mangondo, *Comput. Theor. Chem.*, 2015, **1053**, 60–76.
35. J. H. de Lange, D. M. E. van Niekerk and I. Cukrowski, *J. Comp. Chem.*, 2018, **39**, 2283–2299.
36. E. R. Johnson, S. Keinan, P. Mori-Sánchez, J. Contreras-García, A. J. Cohen and W. Yang, *J. Am. Chem. Soc.*, 2012, **132**, 6498–6506.
37. Gaussian 09, Revision A.02, M. J. Frisch, G. W. Trucks, H. B. Schlegel, G. E. Scuseria, M. A. Robb, J. R. Cheeseman, G. Scalmani, V. Barone, G. A. Petersson, H. Nakatsuji, X. Li, M. Caricato, A. Marenich, J. Bloino, B. G. Janesko, R. Gomperts, B. Mennucci, H. P. Hratchian, J. V. Ortiz, A. F. Izmaylov, J. L. Sonnenberg, D. Williams-Young, F. Ding, F. Lipparini, F. Egidi, J. Goings, B. Peng, A. Petrone, T. Henderson, D. Ranasinghe, V. G. Zakrzewski, J. Gao, N. Rega, G. Zheng, W. Liang, M. Hada, M. Ehara, K. Toyota, R. Fukuda, J. Hasegawa, M. Ishida, T. Nakajima, Y. Honda, O. Kitao, H. Nakai, T. Vreven, K. Throssell, J. A. Montgomery, Jr., J. E. Peralta, F. Ogliaro, M. Bearpark, J. J. Heyd, E. Brothers, K. N. Kudin, V. N. Staroverov, T. Keith, R. Kobayashi, J. Normand, K. Raghavachari, A. Rendell, J. C. Burant, S. S. Iyengar, J. Tomasi, M. Cossi, J. M. Millam, M. Klene, C. Adamo, R. Cammi, J. W. Ochterski, R. L. Martin, K. Morokuma, O. Farkas, J. B. Foresman, and D. J. Fox, Gaussian, Inc., Wallingford CT, (2016).
38. AIMAll (Version 19.02.13), Todd A. Keith, TK Gristmill Software, Overland Park KS, USA, 2019 (aim.tkgristmill.com).
39. A. Müller, *Phys. Lett. A*, 1984, **105**, 446–452.
40. M. A. Blanco, A. M. Pendás and E. Francisco, *J. Chem. Theory Comp.*, 2005, **1**, 1096–1109.
41. P. M. Polestshuk, *J. Comp. Chem.*, 2013, **34**, 206–219.
42. O. Gritchenko, K. Pernal and E. J. Baerends, *J. Chem. Phys.*, 2005, **122**, 204102.
43. I. Cukrowski and P. M. Polestshuk, *Phys. Chem. Chem. Phys.*, 2017, **19**, 16375-16386.
44. F. Cortés-Guzman and R. F. W. Bader, *Coord. Chem. Rev.*, 2005, **249**,633–662.
45. Z. Badri and C. Foroutan-Nejad, *Phys. Chem. Chem. Phys.*, 2016, **18**, 11693–11699.

46. D. W. Turner, C. Baker, A. D. Baker and C. R. Brundle, *Molecular Photoelectron Spectroscopy: A Handbook of He 584 Å Spectra*, Interscience, New York, 1970.
47. K. B. Wiberg, R. F. W. Bader, and C. D. H. Lau, *J. Am. Chem. Soc.*, 1987, **109,** 985–1001.
48. C. Foroutan-Nejad, Z. Badri and R. Marek, *Phys. Chem. Chem. Phys.,* 2015, **17**, 30670–30679.
49. P. L. A. Popelier, *Struct. Bond.,* 2016, **170**, 71–118.
50. E. Francisco, D. M. Crespo, A. Costales and A. M. Pendás, *J. Comp. Chem.,* 2017, **38**, 816–829.
51. V. Tognetti and L. Joubert, *J. Chem. Phys.*, 2013, **138**, 024102–024111.

TOC

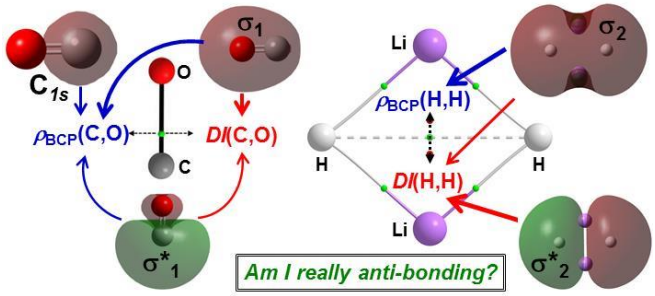

Quantifying contributions to any kind of bond/interaction and diatomic electron delocalization (bond order) made by individual (non)bonding molecular orbitals.